International Journal of Scientific Research in Computer Science, Engineering and Information Technology
© 2016 IJSRCSEIT | Volume 1 | Issue 2 | ISSN : 2456-3307

Bearing Shaft Accuracy as One of Vibration Sources and Industrial Application

Zuzana Murčinková

Department of Technical Systems Design, Faculty of Manufacturing Technologies, Technical University of Košice, Bayerova 1, Prešov, Slovak Republic

ABSTRACT

The paper analyses the bearing shaft surface geometry as one of factors influencing the vibrations values and thus the life of rolling bearings. Any deviation of ideal cylindrical shape of contact surface of bearing shaft and inner bearing ring considerably influence the shape of bearing rolling race. The dimension and geometry accuracy of bearing shaft is very important for intended life and mounting of bearing. Moreover, paper dealt with analytical, numerical approaches for pressed joint and it provides the application to flexoprinting machine for which the presented analyses were made to eliminate high-speed printing vibrations.

Keywords: Interference Fit, Accuracy, Bearing Life, Printing Quality, Vibration

I. INTRODUCTION

The experiences showed there are the unsatisfied customers who despite the fact they buy new or precise bearings, the bearing life is several times or even one/two order/s shorter. Moreover, dissatisfaction is also caused by noisy bearings operation. Furthermore, some of the bearing users decide to use precise bearings that are about 10-times more expensive and they do not achieve satisfaction. Such customers think that the bearings are not of enough quality. The answer is in accuracy but not the accuracy of bearing but the accuracy of bearing shaft.

In generally, the research of various parameters influencing the bearing life was performed to increase the life of usage in different research institutions in the world.

Interference fits on the inner ring of a cylindrical roller bearing can significantly reduce bearing fatigue life [1, 2]. Moreover, interference fits also affect the maximum Hertz stress-life relation. The life factors found in their study ranged from 1.00 (no life reduction) to a worst case of 0.38 (a 62-percent life reduction). Experimental data of Czyzewski showing the effect of interference fit on rolling-element fatigue life determine the shear stress-life exponent [1, 2].

Furthermore, relationships were found between bearing life and internal clearance as a function of ball or roller diameter, adjusted for a load by Oswald, F.B., Zaretsky and E.V., Poplawski J.V. in [3]. They analyzed the variation of loads on the elements of a radially loaded ball bearing. Rolling-element loads can be optimized and bearing life maximized for a small negative operating clearance. Bearing life declines gradually with positive clearance and rapidly with increasing negative clearance [3]. These analyses are focused on internal clearance. Taking into account the influence of fits and thermal gradients Ricci in [4] introduces a procedure for get numerically, accurately and quickly, the static load distribution of a ball bearing under axial and radial loading.

Cao et al. [5] concerned with the variation of interference fit and the preload condition of bearings in a high-speed spindle system. The centrifugal radial expansion deformations due to the centrifugal force also induce the variation of internal clearance which changes of the joint state between the shaft and the bearing. If the internal clearance of the bearing becomes smaller than the specified value, the breakage

of oil film and seizure due to excessive contact stress may lead to the reduction of bearing life, and even spindle vibration and noise [5].

The bearing unit is multi-parameter system and its life is influenced by many parameters. The mentioned research analyses did not involve inaccuracy (dimensional and geometrical) of shafts as a source of larger vibrations and noise resulting in the reduction of bearing life. Our research has been focused on the impact of shaft accuracy on bearing life. The paper focused on dimensional and geometrical inaccuracies that highly modify the bearing life. Moreover, the paper provides the results obtained in the flexoprinting machine where the needle rolling bearings were mounted focusing on radial bearing clearance and related vibrations. The vibration measuring draw connection between the size of the vibration and the accuracy of the bearing shaft, upon which the bearing mounted.

Furthermore, this problem is connected with manufacturing of shaft cylindrical surface. The waviness and other geometrical deviations of manufactured surface are the physical phenomenon caused by dynamic character of cutting process. It can be minimized, but not eliminate. More is discussed in [6-9].

Bearing life is running time of the bearing until the appearance of signs of material fatigue on the contact surfaces of solids of revolution or the races [10]. The bearing life is expressed in terms of the number of millions of revolutions (10^6 min^{-1}) of one race relative to another or in terms of working hours.

The basic equation of bearing life L calculation is:

$$L = \left(\frac{C}{F}\right)^p \qquad (1)$$

where C is base dynamic load rating (in catalogues), it means the load that responds to a basic bearing life of million revolutions, N, F is applied load, N, and p is exponent that is chosen in accordance with the outcomes of experiments – for ball bearings p=3, for roller bearings p=10/3. The load F is substituted by F_e, equivalent dynamic load. For more detailed life calculation see more in [11-13].

The mentioned equation (1) considers the low changing, symmetrical and centric load; for radial bearings it assumes only radial load, the rotating inner ring, the not moving outer ring, standard bearing steel, rotational frequencies, etc. For material or operating conditions different from the standards ones as well as increased safety requirements and to take into account special bearing properties, the corrected bearing life is determined.

The real service conditions of bearings may strongly change the theoretically estimated bearing life. We can involve correcting coefficient a and then the equation (1) has form:

$$L = a\left(\frac{C}{F}\right)^p \qquad (2)$$

where a is coefficient in range 0.1÷10 according to experiences and measuring depending on special bearing properties and operating conditions. The range of a is large and significantly influence the bearing life.

II. METHODS AND MATERIAL

To demonstrate the importance of bearing shaft accuracy, we made the numerical simulation of pressed joint to find the relation between accuracy of bearing shaft or bearing case and inner or outer rolling race.

We analyze the pressed joint (Fig. 1) of bearing shaft and inner bearing ring. The aim of analysis and numerical simulation is to find:

- outer radial displacement Δr_3^{II} of inner race; it means the increase of inner rolling ring radius depending on ring thickness and interference,
- inner radial displacement Δr_2^{II} (Δr_2^{I}) of the inner rolling ring (bearing shaft radius),
- influence of bearing shaft roundness (circularity) on outer radial displacement Δr_3^{II} after mounting,
- influence of bearing shaft surface micro-geometry on outer radial displacement Δr_3^{II} after mounting.

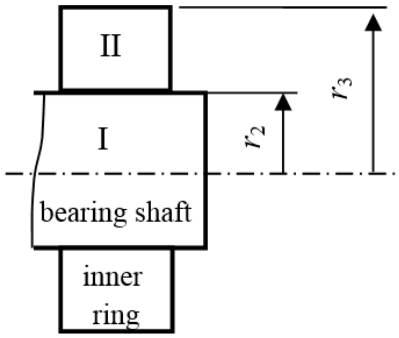

Figure 1. Pressed joint - schema

Let's consider interference fit in hole-basis system of fits Ø100H7/p6. The maximal and minimal dimensions of hole and bearing shaft and interferences are known. The roundness for any fit is IT/2. Roundness tolerance specifies a tolerance zone bounded by two concentric circles within which each circular element of the surface must lay [10]. The roundness tolerance depicts Fig. 2 (Fig. 2, right – measured roundness, real shaft profile).

For example, the tolerance range for ring hole is 0.035 mm (0.0175 mm for radius). The roundness tolerance from mechanical engineering tables is 0.016 mm for IT7. The roundness tolerance must be less than the dimension tolerance. IT/2 is involved for roundness tolerance.

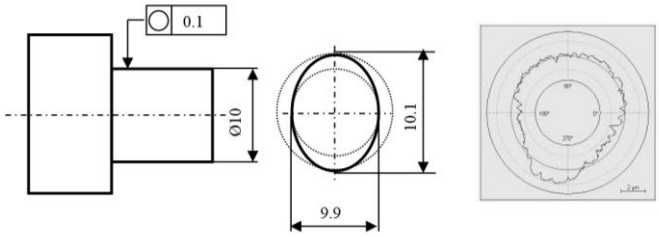

Figure 2. Roundness tolerance

To simulate the influence of bearing shaft inaccuracy, the no ideal "cylindrical" contact surfaces are substituted by elliptical shape. The real cross-section of bearing shaft and ring may have various shapes and dimensions depending on turning condition, but they must be within tolerance size and roundness range.

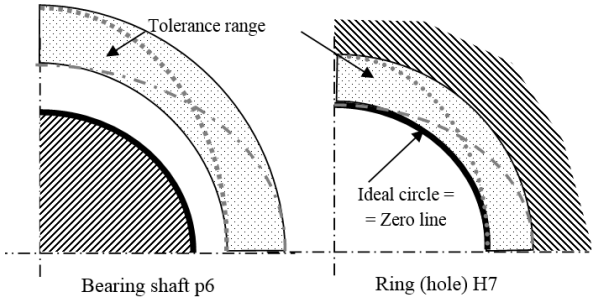

Figure 3. Dimensional and geometry accuracy

Figure 3 analyses possible variants of dimensional and geometry accuracy. The ellipses of dashed, dash-dotted, dotted lines represent extremely variants of cross-sections.

Figure 4 depicts the two extreme combinations that are made by the combination of various cross-section described in Fig. 3. Every other combination than that shown in Fig. 4 is the same but revolved by 90°. The extreme case selected for numerical simulation is the variant 2 in Fig. 4 because of largest and lowest interference with maximum and minimum roundness.

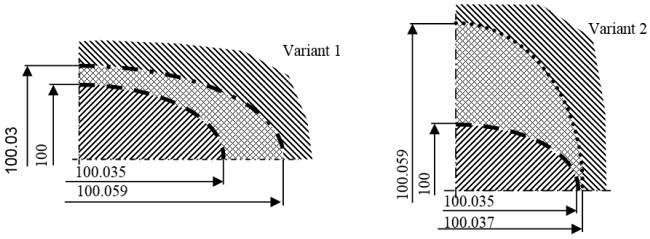

Figure 4. Variants

III. RESULTS AND DISCUSSION

A. Analytical Calculation

The radial σ_r, tangential σ_t and contact p_2 stress are analytically calculated as pressed joint that calculation is induced according to a theory of thick-wall pipes [14, 15]. Despite the fact that in most cases we consider the bearing ring as thin-walled. Criterions between thin and thick walled pipes are different according to several authors. We decided to use the dimensions that are on the border between them (r_2 = 50 mm, r_3 = 60 mm). Following formulas are according to [14-16].

Tangential and radial stress:

$$\sigma_{t,r}(r) = A \pm \frac{B}{r^2} \qquad (3)$$

where *A*, *B* are integral constants calculated from boundary conditions, *r* is radius.

Contact pressure p_2:

$$p_2 = \frac{\delta\ E}{2\,r_2}\ \frac{\left(r_3^2 - r_2^2\right)}{2\ r_3^2} \tag{4}$$

where δ is interference, E is Young's modulus of elasticity.

Radial bearing shaft displacement Δr_2^{I} (decrease of original bearing shaft radius):

$$\Delta r_2^{\mathrm{I}} = \frac{p_2\ r_2}{E}(1-\mu) \tag{5}$$

where μ is Poisson's ratio.

Radial ring displacement Δr_2^{II} (increase of original bearing shaft radius):

$$\Delta r_2^{\mathrm{II}} = \frac{p_2\ r_2}{E}\left(\frac{r_2^2 + r_3^2}{r_3^2 - r_2^2} + \mu\right) \tag{6}$$

To control results we can use:

$$\frac{\delta}{2} = \left|\Delta r_2^{\mathrm{I}}\right| + \Delta r_2^{\mathrm{II}} \tag{7}$$

Results are in column "Analytical" of Table I.

B. Numerical Results

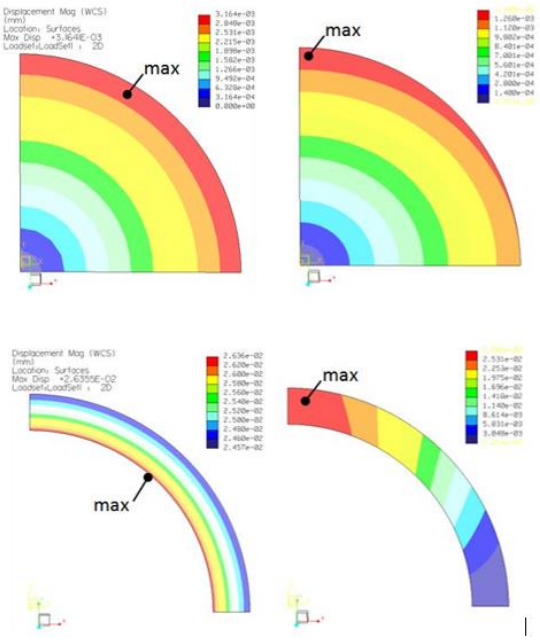

Figure 5. Displacements of ideal (left) and elliptical contact surfaces

The numerical model is equivalent of variant 2 in Fig. 4. One-quarter model is modelled because of symmetrical boundary conditions. The interference fit is a type of model for non-linear analysis with the contact region in the contact surface. The computational method is Newton-Raphson method. Five loading intervals and localized mesh refinement with convergence on contact forces are used for computation. Displacement distribution in case of ideal and unideal cylindrical surfaces of bearing shaft and ring is in Fig. 5. Results are in column "Numerical" of Table I.

Table 1 provides results and their comparison. The match in the percentage of the difference between analytical and numerical solutions is very good. The largest difference is in the case of contact pressure – 2.94%. The numerical model is reliable.

TABLE I.
RESULTS COMPARISON FOR IDEAL CYLINDRICAL SURFACES

	Analytical model	**Numerical model**	**Difference [%]**
p_2 (MPa)	18.03	18.56	2.94
Δr_2^{I} (mm)	0.00315	0.0031439	0.19
Δr_2^{II} (mm)	0.0263	0.0263551	0.21
$\sigma_{\mathrm{t}}^{\mathrm{II}}(r = r_2)$ (MPa)	99.82	100.309	0.49
$\sigma_{\mathrm{t}}^{\mathrm{II}}(r = r_3)$ (MPa)	81.81	81.998	0.23

Figure 6 shows the radial displacement Δr_3^{II} of inner race in dependence on the thickness of the ring. The interference and bearing shaft dimension are constant. The calculation is for Ø100H7/p6. The radial displacement Δr_3^{II} is important quantity. It influences radial clearance of bearing. The distance between red and blue lines is the same. It responds the value of interference. Changing the radius r_3, the thickness of the ring is larger (the r_2 is constant) and this change directly influences the radial displacement r_3 (green line). "Cylindrical" surface with radius r_3 is intended rolling race. In case the radius (diameter) ratio of ring and bearing shaft is 1.05:1 than radial displacement Δr_3^{II} is 98% of interference. In case the radius (diameter) ratio of ring and bearing shaft is 2:1 than

radial displacement Δr_3^{II} is 71.4% of interference. The larger ring thick, the larger radial bearing shaft displacement Δr_2^{I}, and lower radial displacement Δr_3^{II}. But in case of larger ring thick the contact pressure becomes larger.

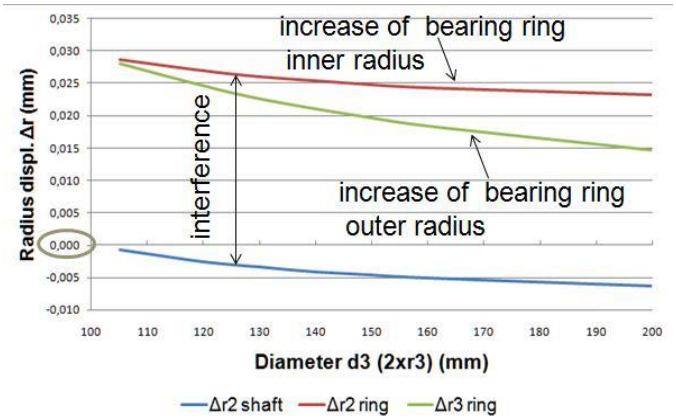

Figure 6. Radius displacement vs. ring thickness

Figure 7 presents increasing of contact pressure with increasing the ring thickness.

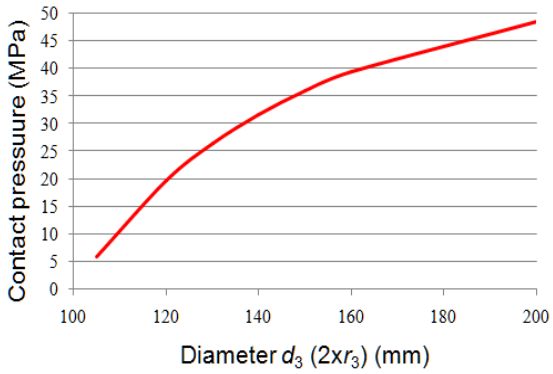

Figure 7. Contact pressure vs. ring thickness

We have to realize that radial displacement Δr_3^{II} is 98 – 71.4% of interference in dependence of ring thickness. It is the reason why any deviation of the ideal cylindrical shape of contact surfaces significantly appears on the shape of rolling ring and consequently the vibrations and bearing life. So, the dimension and geometry accuracy of bearing shaft strongly influence deviations of ideal rolling race shape.

Figure 8 shows the influence of different value of interferences on radial displacements r_2 and r_3. Interference fits are following: Ø100 H7/k6, Ø100 H7/p6 and Ø100 H7/s6. It is evident that radial displacement Δr_3^{II} is about 92% of interference.

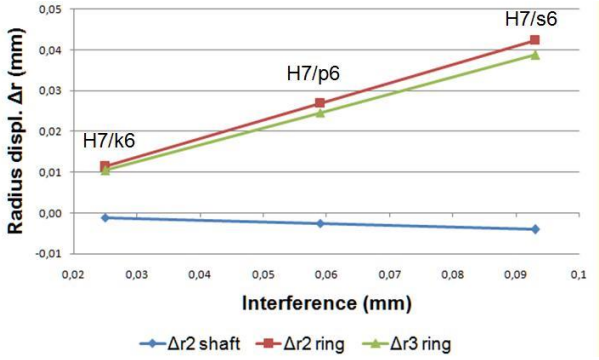

Figure 8. Radius displacement vs. interference

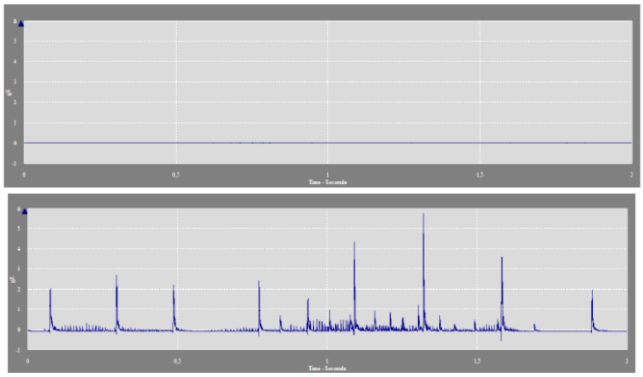

Figure 9. Bearing before (up) and after damage (EnvAcc up to 20kHz)

Figure 9 shows time records of 2 seconds for the same bearing before and after damage. Upper time record in Fig. 9 provides no symptoms of seizing, metal contact, wearing, abrasion, damage contact surface. Signal is without high amplitudes. Time record situated lower in Fig. 9 provides no-periodical peeks with high amplitudes that indicate heavy bearing failure.

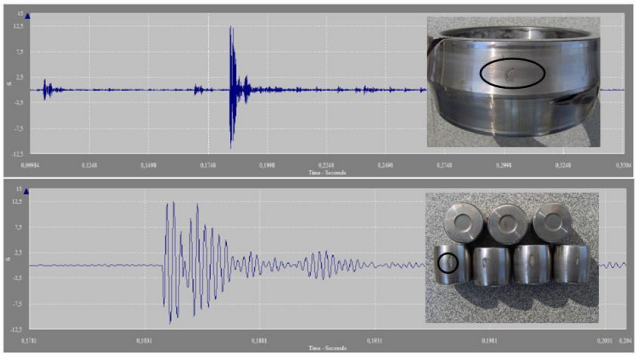

Figure 10. Time record

Figure 10 shows time record with a typical signal of seizing and the metal contact. The inner bearing ring and solids of revolution with pitting are showed.

IV. INDUSTRIAL APPLICATION

Flexography is a form of the printing process using the flexible image plates on which the printing areas are above the non-printing areas. Flexographic printing is a modern printing technology. The different printing plates are for different colours. The rotary principle of printing enables the simple control of printing speed. The printed flexible films (bags, cartons, labels etc.) are intended for packaging in food and chemical industry.

Fig. 11 shows the scheme of the printing section of the flexographic printing machine. The flexible thin plastic (film) passes the individual printing positions and it enters the drying section. The each printing position involves plate and raster (anilox) cylinders with the inking unit of individual colour. The raster cylinder has small holes (cells) or grooves which are being filed by colour ink while rotation. Then the ink is applied on relief of plate. The profile of plate is imprinted on flexible film that is passing to another printing position with another plate and colour. There are the 4-, 6- 8-, 10-coloured printing machines with different printing width (800-1870 mm) and different printing speeds (100-1000 m/min).

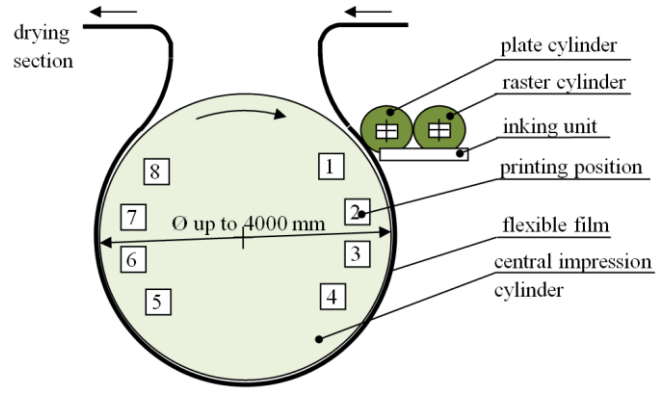

Figure 11. Scheme of printing section

Dynamic impact in printing is caused by impact between the plate cylinder and central impression cylinder – its external cylindrical surface. The high vibration of plate cylinder causes the low quality of printing due to gaps or overlapping colours in case of the multicoloured pattern (image).

The measurements were made in cooperation with Technická diagnostika, Ltd. to determine the forces or localities that causing repeated impact, the envelope measuring method was used. Acceleration Enveloping (Fig. 12) detects repeating vibration signals in high-frequency range. The same method is used for analysing of roller bearings and teeth frequencies where the source of repeating signal is crossing the damaged place by rotational motion [17-19].

Acceleration Enveloping confirms that repeating impact is caused by straight edges of the pattern at plate cylinder into central cylinder. At the same time the mentioned method allows identifying the time of damping (Fig. 12). While vibration is being damped, the area of the flexible film is without colour. This lower class quality part of printing can be visible only by use of a microscope. But if the higher printing speed is used, the impact force is higher, the time of damping is longer and quality of printing is worse. Such printing conditions produce film with uncoloured areas that are visible by eyes and/or individual colours are overlapped.

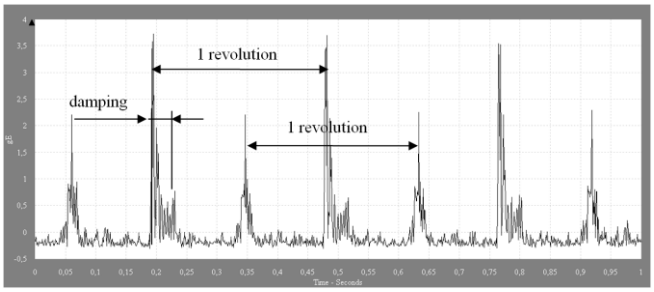

Figure 12. Acceleration Enveloping

There are more or less suitable reliefs of printing plates in term of vibrations formation. The most difficult printing design involves the straight rising edges that cause the creation of higher impacts what directly influence the printing speed. The straight rising edge is the edge that is perpendicular to film winding direction and it is at least appropriate. The more appropriate are sloping edges.

The magnitude of vibrations is also influenced by the material of plate situated on the plate cylinder. The plates are made of four kinds of rubber differ by elasticity, wearing and stability of printing quality.

A. Component joints accuracy and vibrations

The next section describes the problem solution through vibrodiagnostic control and improving the accuracy of mounting and individual machine parts in component joints. The measured points for monitoring dynamic signal were following: printing position 1-8; plate and raster cylinders; horizontal and vertical

direction of vibrations; operator and drive sides. Altogether 64 (8x2x2x2) outputs of measured points are for evaluation. To decrease the vibration, the following arrangement work was made on selected flexographic printing machines:

- exchange of bearing mounting at operator (OS) and drive side (DS),
- setting of radial clearance of main needle bearings by selection of appropriate bearing shaft tolerance,
- control of radial run out of cylinders surface and tolerance of concentricity compared with axes of bearing shaft bearing cylinders.

The correct operation of flexographic printing machines is strongly influenced by radial clearance of needle bearing - RNA 6913, RNA 6916. The magnitude of radial clearance (lower, normal, higher) influences the size of the loaded area in bearing; it means that the smaller clearance, the more solids of revolution carry the radial load. Thus, the load of each solid of revolution is lower. Moreover, the ability of damping of dynamic excitation and vibrations generated by printing process is influenced by radial clearance. The optimal function of needle bearing is guaranteed by a producer if the recommended radial clearance in range 30-50 μm is used.

The standard needle bearings are produced with normal radial clearance. The inner races are thin-walled and the required clearances are achieved by bearing shaft tolerance (k5, h5, g6, f6). In case of special inner bearing race (for example wider bearing for axial displacement of cylinder) it is needful to choose tolerance of bearing shaft and tolerance of race surface diameter. The final measure of race surface after mounting (fixing the inner race on the bearing shaft) should guarantee working clearance in recommended range of 30-50 μm. In such case, it is suitable to grind the race surface and set the required measure after mounting on the bearing shaft (cylinder).

The estimation of measured machine elements state is according to standard STN ISO 10816-3 (Slovak Technical Standard modified according to the International Organisation for Standardization): Measuring of vibrations of revolving machines that introduces the recommended limits of Warning and Danger of summing vibrations (Table 2).

TABLE II.

ALARMS LIMITS AND MEASURED VALUES BEFORE AND AFTER ARRANGEMENT WORK

			Velocity [mm/s]	**Acceleration [g]**	**Time Acc [g]**	
Alarm 1:Warning			2.8	0.15	1.5	
Alarm 2: Danger			4.5	0.25	2.0	
before	OS position 8	HD	*5.84*	*0.34*	*2.8*	Alarm 2: Danger
		VD	1.78	0.15	*2.0*	
	DS position 8	HD	*6.94*	*0.28*	*2.2*	
		VD	1.56	0.10	*1.8*	
after	OS position 8	HD	1.32	0.10	1.4	No alarm
		VD	1.00	0.10	1.2	
	DS position 8	HD	1.04	0.08	0.8	
		VD	0.59	0.09	1.0	

The measured results in Table 2 show the vibrations in the horizontal direction (HD) are larger up to 4.5-times than in vertical direction (VD). Comparing the measured of vibrations values before arrangement work and the measured values at the same locations after arrangement work, i.e. after change the bearings and control of the rotational accuracy of cylinders, it is obvious that after arrangement work strong vibrations decreasing 43 - 85% of vibration velocity and thus dynamic excitation of the printing position. Such results increased the quality of printing.

V. CONCLUSION

The paper provides analytical, numerical and experimental results of unideal and inaccurate contact surfaces of bearing shaft and inner bearing ring. Deviation of an ideal cylindrical shape of contact surfaces considerably influences the shape of bearing rolling race and radial clearance of bearing. The calculations show that radial displacement Δr_3^{II} - the increase of inner rolling ring is more than 70% of interference. It means the inaccuracy of bearing shaft geometry is “copied” 70% - 90% into rolling race by press assembling and thus is source of unwanted vibrations that shortening the bearing life and influencing the precision of machine operation.

The radial clearance and accuracy of bearing shaft/cylinder have the main role in dynamic excitation resulting in unwanted vibrations of printing cylinder of flexoprinting machine as well as character of printing plate relief. The printing process is influenced also by other factors, for example used materials, not only by machine arrangement.

In next research, we will analyse the waviness (number, high) of bearing shaft surface and influence to vibration and bearing life.

VI.REFERENCES

[1] Oswald, F.B., Zaretsky E.V. and Poplawski J.V. 2009. Interference-Fit Life Factors for Roller Bearings, Tribology Transactions, 52 (4), pp. 415-426.

[2] Oswald, F.B., Zaretsky, E.V. and Poplawski J.V. 2010. Interference-Fit Life Factors for Ball Bearings, NASA/TM—2010-216913.

[3] Oswald, F.B., Zaretsky and E.V., Poplawski J.V. 2012. Effect of Internal Clearance on Load Distribution and Life of Radially Loaded Ball and Roller Bearings, NASA/TM-2012-217115.

[4] Ricci, M.C. 2009. Internal Loading Distribution in Statically Loaded Ball Bearings, Subjected to a Combined Radial and Thrust Load, Including the Effects of Temperature and Fit, World Academy of Science, Engineering and Technology 33, pp. 290-298.

[5] Cao H., Holkup T., Chen, X. and He, Z. 2012. Study of characteristic variations of high-speed spindles induced by centrifugal expansion deformations, Journal of Vibroengineering, 14 (3), pp. 1278-129.

[6] Tlusty, J. 1978. Analysis of the state of research in cutting dynamics, Annals of the CIRP, pp. 583-589.

[7] Vela-Martínez, L. et al. 2008. Analysis of compliance between the cutting tool and the workpiece on the stability of a turning process, International Journal of Machine Tools & Manufacture 48, pp.1054–1062.

[8] Siddhpura, M. and Paurobally, R. 2012. A review of chatter vibration research in turning. International Journal of Machine Tools & Manufacture, 61, pp. 27–47.

[9] Vasilko, K. and Mádl, J. 2012. "Teorie obrábění (Theory of machining)", University of J.E. Purkyně in Ústí nad Labem, Czech Republic.

[10] "Springer Handbook of Mechanical Engineering " 2009. ed. by Grote, K.H., Antonsson, E.K. (Eds.), Springer-Verlag Berlin Heidelberg.

[11] Bolek, A., Kochman, J. et al. (1989), "Částí strojů, 1. svazek (Machine Elements, 1st part)", SNTL, Prague, Czech Republic.

[12] Fröhlich, J. 1978. "Technika uložení s valivými ložisky (Bearing Housing Design)", SNTL/ALFA, Prague, Czech Republic.

[13] Klebanov, B. M., Barlam D.M. and Nystrom F.E. 2007. "Machine Elements: Life and Design", CRC Press.

[14] Murčinková, Z. 2013. "Pružnosť a pevnosť I., Teória a príklady. (Elasticity and Strength of Materials I., Theory and exercises)", Faculty of Manufacturing Technologies, Technical university of Košice, Prešov, Slovak Republic.

[15] Trebuňa, F., Šimčák, F. and Jurica, V. 2001. "Príklady a úlohy z pružnosti a pevnosti II. (Examples and Problems of Elasticity and Strength II.)", Vienala, Košice, Slovak Republic.

[16] Leckie, F.A. and Dal Bello, D.J. 2009. "Strength and Stiffness of Engineering Systems", Springer Science+Bussiness Media.

[17] Murčinko, J. 2012. Analysis of dynamic effects of mulching machine, In: IMEF 2012, Proceeding of 5th International Mechanical Engineering Forum: June 20th - June 22nd 2012, Czech University of Life Sciences, Prague, pp. 700-705.

[18] Murčinko J. and Murčinková Z. 2012. On-line monitoring system applied to explosive conditions of printing machine dryers, in: Risk Analysis, 44 (8), 305-316.

[19] Howard, I. 1994. A Review of Rolling Element Bearing Vibration "Detection, Diagnosis and Prognosis", DSTO Aeronautical and Maritime Research Laboratory, Melbourne.